Journal of Alloys and Compounds 690 (2017) 376–380

Contents lists available at ScienceDirect

Journal of Alloys and Compounds

journal homepage: http://www.elsevier.com/locate/jalcom

Abnormal migration of twin boundaries in rolled AZ31 alloy containing intersecting $\{10\bar{1}2\}$ extension twins

Huicong Chen [a, b], Tianmo Liu [a, b, *], Shihua Xiang [a, b], Yanxiang Liang [a, b]

[a] *College of Materials Science and Engineering, Chongqing University, Chongqing 400030, China*
[b] *National Engineering Research Center for Magnesium Alloys, Chongqing University, Chongqing 400030, China*

ARTICLE INFO

Article history:
Received 9 May 2016
Received in revised form
15 August 2016
Accepted 17 August 2016
Available online 20 August 2016

Keywords:
Magnesium alloy
Intersecting $A10\bar{1}2A$ twins
Twin boundary migration
Twin variant selection
Schmid factor

ABSTRACT

Twin boundary (TB) migration under the condition of the interaction between different {10–12} twin variants with a high misorientation of 60.4° was investigated by using in-situ electron backscattered diffraction technique combined with Schmid factor analysis. It was found that TBs would continue to migrate when the sides of intersecting twin bands enclose an acute angle, but cease to migrate on the sides making an obtuse angle. Besides, due to the twin-twin interaction, half locked and entirely locked twin boundaries occurred as deformation progressed. Moreover, strain accommodated by double twin and new active twin was found at further imposed strain in current study.

1. Introduction

The formation of twins and the mobility of twin boundaries play an important role in strain accommodation during plastic deformation of hexagonal close packed (hcp) metals and, in general, of low-symmetry crystals [1–4]. Among the several types of deformation twins that have been reported in deformed Mg and its alloys, $\{10\bar{1}2\}\bar{1}011$ extension twin is the most common one, which can accommodate the tension strain along c axis [5–8]. Theoretically, six equivalent $\{10\bar{1}2\}$ twinning variants [2,6,7,9] can be activated under favorably applied stress [9–11]. Therefore, twin–twin intersection between different $\{10\bar{1}2\}$ twin variants is inevitable during plastic deformation, which has attracted extensive attention [5,6,10].

Due to the development of internal stresses during twin-twin interaction, higher stress [12] for the twin propagation arises and thus twinning growth could be retarded and then new twins would be activated to accommodate the further imposed strain even at the late stage of deformation [10]. It is worth mentioning that only the interactions where twin variants are with a high misorientation angle can significantly impede twinning growth [8,10]. Different twin-twin interaction types were systematically reviewed by Yu et al. [5] and they proposed that one twin could transmit into the other by secondary twin in crossed area under some special loading conditions. The formation of twin–twin boundary (TTB) plays a critical role in “apparent crossing” [5] twin structures and the pile-up of TTB dislocations could cause a tilt of the crystal in the intersection region. Via transmission electron microscopy (TEM) analysis, Sun et al. [6] confirmed such TTB shows a very large deviation from the original coherent TB and it implies that TTB interaction influences the structural features of the original coherent TB. Recent high resolution transmission electron microscopy (HRTEM) results [13] indicated that the coherence of TBs would be greatly damaged by severe TB dislocation interaction and this interaction might lead to curving of TBs and the strain hardening [14]. Thereafter, Shi et al. [15] investigated four typical twin-twin structures and they found that intersection between different twin variant pairs could retard the twin growth and then trigger new twins near intersection region. They also mentioned that TTB migration is an important cause to prohibit twins for further propagate and growth, but they did not expatiate on this point. Some similar findings can be found in other studies [5,10]. Moreover, numerous characterizations were conducted to reveal the microstructural features of this interaction by means of electron backscattered diffraction (EBSD) [5,16–19] and TEM analysis [6,14,17]. These observations are mainly focused on some common characteristics,

---

[*] Corresponding author. College of Materials Science and Engineering, Chongqing University, Chongqing 400030, China.

E-mail addresses: hcchen@cqu.edu.cn (H. Chen), tmliu@cqu.edu.cn (T. Liu).

http://dx.doi.org/10.1016/j.jallcom.2016.08.154

such as twin–twin boundaries (TTBs), twinning tips and twinning penetration. However, few studies involve the migration behavior of twin boundaries under the influence of twin-twin interactions.

Recently, we observed some peculiar migration of TBs under the influence of the intersecting $\{10\bar{1}2\}$ twin variants with the deformation proceeding. These TBs were entirely locked or half locked by the intersecting area (IA) or crossed twin. Additionally, the blocked sides of both twins made an obtuse angle while the mobile sides enclosed an acute angle, which was similar with the early observation by TEM in the body centered cubic (bcc) metal [20]. Besides, the double twin (DT) was active in the intersecting area, pinning the TBs and reducing their mobility. New twins were also activated to accommodate further deformation.

In this study, in situ EBSD was performed to verify these findings. Therefore, we explored the migration behavior of TBs in grains containing intersecting $\{10\bar{1}2\}$ extension twins. Moreover, Schmid factor (SF) was computed to analyze the twin variant selection during the deformation.

2. Experimental section

Investigations were carried out on a commercial hot-rolled sheet of magnesium alloy AZ31 (chemical composition (wt.%): 3% Al, 1%Zn, 0.5Mn%,0.0075%Si, 0.007%, 0.0003%Fe, 0.00025%Cu, Mg balanced) with a thickness of 30 mm. Samples with a dimension of 3 mm × 4 mm × 5 mm (ND × TD × RD) were wire-cut from the sheet and subjected to heat treatment for 2 h at 400 °C to produce the equiaxed microstructure with an average grain size of 30 μm as shown in Fig. 1(a). Here, the ND, TD, RD refer to normal direction, transverse direction and rolling direction, respectively. It is also important to note the starting texture of these samples, shown by the basal and prismatic pole figures in Fig. 1(b), which present the typical fiber texture associated with prior hot rolling, having a substantial scatter of the c-axis direction around ND about 0–25°. For EBSD test, the specimen surface was mechanically ground followed by a final electrochemical polish in AC2 (800 ml ethanol + 100 ml propanol + 18.5 ml distilled water + 10 g hydroxyquinoline + 75 g citric acid + 41.5 g sodium thiocyanate + 15 ml perchloric acid).

Compressive steps to different true strain levels (0%, 3%, 7.5%) along the RD were conducted at a strain rate of 10^{-3} s^{-1} and ambient temperature. Before and after each deformation step, EBSD measurements were performed on a JEOL JSM-7800F scanning electron microscope equipped with an EBSD camera and the AZtec acquisition software package (Oxford Instruments), using a step size of 0.2 μm.

3. Results and discussion

As reviewed above, a grain could twin on any one of six possible $\{10\bar{1}2\}$ planes, forming six variants, here denoted as Vi (i = 1–6). Fig. 2(a) illustrates orientation relationships of six $\{10\bar{1}2\}$ twin variants in crystallography coordinate system. It is known that all six twin variants are possible to be activated simultaneously under tension along c-axis, with an equal SF around 0.499 [10,21,22]. Accordingly, three different misorientation relationships [23] can be achieved between different variants and these are 60°$10\bar{1}0$ between V1 and V2, 60.4°$8\bar{1}\bar{7}0$ between V1 and V3, 7.4°$1\bar{2}10$ between V1 and V4 as illustrated in the crystallographic relationships of Fig. 2(b). In general, only one relationship, i.e. 7.4°$1\bar{2}10$ occurs when compression is performed perpendicular to c-axis because this twin variant pair is adjacent to the loading axis and has the highest SF value [10]. However, above calculation is based on assumption that experimental materials have an ideal fiber texture. Actually, there is a substantial scatter of the initial fiber around ND about 0–25° as shown in Fig. 1(a). Therefore, for compression along RD conducted on a hot rolled AZ31, primary active variants would be more profuse and the interplay of different twins will occur in a single grain as the deformation proceeds.

Fig. 3 shows the partial compressive curve of the sample compressed to 7.5% along the RD and corresponding EBSD maps at different strains. The curve exhibits a typical feature of $\{10\bar{1}2\}$ twinning-dominated deformation, i.e. a sigmoidal shape. The microstructure evolution is revealed by three insets (a), (c) and (e), which illustrate the nucleation and propagation of twins with deformation progressing. Besides, when the sample is compressed to the true strain of 3%, intersecting twins (belonging to different variants) is observed with a high misorientation angle around 60° (theoretically, 60.4°), which would impact the twinning behavior at further imposed strain as shown in Fig. 3(e). The details are discussed below.

To reveal the migration of TBs clearly, the enlarged partial maps with different strain levels in a particular grain are redrawn in Fig. 4. No twins are found in the starting material as shown in the initial microstructure picture (Fig. 3(a)). When 3% true strain is imposed to the sample, profuse twinning bands appear in the selected grain as shown in Fig. 4(a). Two different types of $\{10\bar{1}2\}$ twins can be ascertained by the crystallographic relationships between the matrix grain and the twin bands in Fig. 4(e). Here, different twinning lamellas are labeled as Ti (i = 1–13) and the matrix is marked by M. All possible twin variants and their SFs are listed as Table 1. Based on the SF analysis, the selected twins T (1–5) correspond to the variant V6, whose SF was 0.403, while twins T

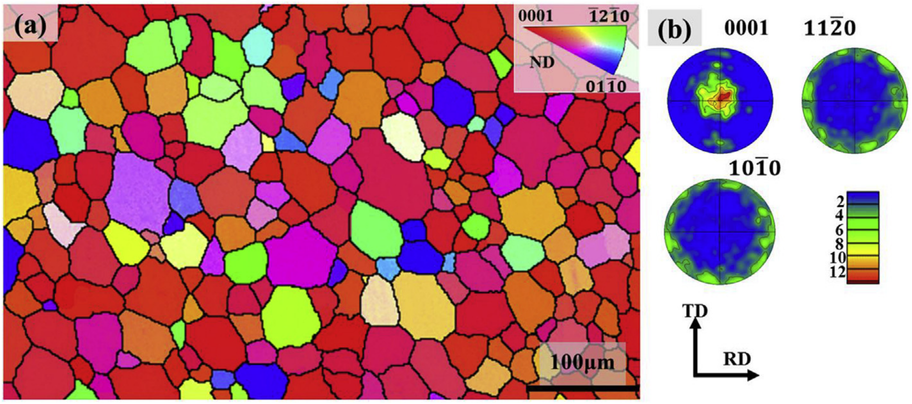

Fig. 1. (a) EBSD map of the initial material, (b) $\{0001\}$, $\{11\bar{2}0\}$ and $\{10\bar{1}0\}$ pole figures from (a).